Mutations in Either Nucleotide-Binding Site of P-glycoprotein (Mdr3) Prevent Vanadate Trapping of Nucleotide at Both Sites†

Ina L. Urbatsch, Lucille Beaudet, Isabelle Carrier, and Philippe Gros*

Department of Biochemistry, McGill University, Montréal, Québec, Canada, H3G 1Y6

Received November 14, 1997; Revised Manuscript Received January 29, 1998

ABSTRACT: Vanadate trapping of nucleotide and site-directed mutagenesis were used to investigate the role of the two nucleotide-binding (NB) sites in the regulation of ATP hydrolysis by P-glycoprotein (mouse Mdr3). Mdr3, tagged with a hexahistidine tail, was overexpressed in the yeast *Pichia pastoris* and purified to about 90% homogeneity by Ni-affinity chromatography. This protocol yielded purified, reconstituted Mdr3 which exhibited high verapamil stimulation of ATPase activity with a V_{max} of 4.2 μmol min^{-1} mg^{-1} and a K_M of 0.7 mM, suggesting that Mdr3 purified from *P. pastoris* is highly functional. Point mutations were introduced into the core consensus sequence of the Walker A or B motifs in each of the two NB sites. The mutants K429R, K1072R (Walker A) and D551N, D1196N (Walker B) were functionally impaired and unable to confer cellular resistance to the fungicide FK506 in the yeast *Saccharomyces cerevisiae*. Single and double mutants (K429R/K1072R, D551N/D1196N) were expressed in *P. pastoris,* and the effect of these mutations on the ATPase activity of Mdr3 was characterized. Purified reconstituted Mdr3 mutants showed no detectable ATPase activity compared to proteoliposomes purified from negative controls (<5% of wild-type Mdr3). Vanadate readily induced trapping of 8-azido-nucleotide in the wild-type enzyme after a short 10 s incubation, and specific photolabeling of Mdr3 after UV irradiation. No such vanadate-induced trapping/photolabeling was observed in any of the mutants, even after a 60 min trapping period at 37 °C. Since vanadate trapping with 8-azido-ATP requires hydrolysis of the nucleotide, the data suggest that 8-azido-ATP hydrolysis is dramatically impaired in all of the mutant proteins (<0.3% activity). These results show that mutations in either NB site prevent single turnover and vanadate trapping of nucleotide in the nonmutant site. These results further suggest that the two NB sites cannot function independently as catalytic sites in the intact molecule. In addition, the N- or C-terminal NB sites appear functionally indistinguishable, and cooperative interactions absolutely required for ATP hydrolysis may originate from both sites.

Multidrug resistance (MDR)[1] is a major limitation to the successful chemotherapeutic treatment of many human tumors and is often associated with the overexpression of P-glycoprotein (Pgp, *1*). Pgp is an integral membrane phosphoglycoprotein that functions as an energy-dependent drug efflux pump to reduce intracellular drug accumulation in resistant cells (*2*, *3*). Pgp-mediated drug transport is strictly ATP dependent (*4*, *5*) and may be mechanistically related to the phospholipid translocase activity demonstrated for Pgp in normal tissue (*6*, *7*). Pgp is composed of 12 transmembrane (TM) domains and 2 nucleotide-binding (NB) domains with characteristic consensus Walker A (GCGKS) and B (ILLLD) sequence motifs, which have been described in a number of ATP-binding proteins and ATPases (*8*). These structural features are grouped into two symmetrical and homologous halves (6 TM, 1 NB) which together define a large protein superfamily known as the ABC (ATP Binding Cassette) family of membrane transporters (*9*). In addition to the three rodent (Mdr1, Mdr2, Mdr3) and two human Pgp isoforms (MDR1, MDR2), some of the best studied ABC transporters include the multidrug resistance protein (MRP) which transports glutathione and glucuronide adducts (*10*), the CFTR chloride channel in which mutations cause cystic fibrosis in humans (*11*, *12*), the sulfonylurea receptor (*11*), and several other members in eukaryotes and prokaryotes (*13*, *14*). In the case of Pgp, epitope mapping studies of proteolytic peptides photolabeled with drug analogues (*15*) and genetic studies of Pgp mutants with altered substrate specificity (*16*) have indicated that TM regions are responsible for substrate binding and recognition. On the other hand, ATP binding and hydrolysis to energize transport has been shown to be mediated by the two NB sites of Pgp (*17*,

† This work was supported by research grants to P.G. from the Medical Research Council of Canada. P.G. is an International Research Scholar of the Howard Hughes Medical Institute and is a Career Scientist of the Medical Research Council of Canada.

* To whom correspondence should be addressed at the Department of Biochemistry, McGill University, 3655 Drummond St., Room 907, Montréal, Québec, Canada, H3G 1Y6. Phone: 514-398-7291. FAX: 514-398-2603. E-mail: gros@medcor.mcgill.ca.

[1] Abbreviations: ABC, ATP-binding cassette; *AOX1*, alcohol oxidase-1; CFTR, cystic fibrosis transmembrane conductance regulator; DM, *n*-dodecyl β-D-maltoside; DTT, dithiothreitol; EACA, ϵ-amino-*n*-caproic acid; L-PC, L-α-lysophosphatidylcholine; MDR, multidrug resistance; Mdr3, mouse *mdr3* P-glycoprotein; MRP, multidrug resistance-associated protein; *mut*^{s}, methanol utilizing slow; NB site, nucleotide-binding site; NB1, N-terminal nucleotide-binding site; NB2, C-terminal nucleotide-binding site; Pgp, P-glycoprotein; PMSF, phenylmethylsulfonyl fluoride; RT, room temperature; SDS−PAGE, sodium dodecyl sulfate−polyacrylamide gel electrophoresis; TM, transmembrane domain; WT, wild-type.

S0006-2960(97)02800-6 CCC: $15.00
Published on Web 03/10/1998

18). Coupling of ATP hydrolysis to drug transport is evident from transport studies in membrane vesicles and purified reconstituted Pgp-liposomes (*4, 5*), and is also apparent from drug stimulation of ATPase activity seen in plasma membrane preparations (*19, 20*) and purified reconstituted Pgp (*21*−*26*).

The precise role of the two Pgp NB sites in this drug-stimulatable ATPase activity and the catalytic cycle involved at one or the other site are not fully understood. Mutations at the key lysine residue in the Walker A motif (GCG**K**S) of each or both NB sites of Pgp have been previously shown to completely abolish Pgp function in mammalian cells (*27, 28*). In purified reconstituted human MDR1, mutations at the corresponding positions (K433M, K1076M) abolished verapamil-stimulated ATPase activity (*24*). Additional photoaffinity labeling studies with 8-azido[α-^{32}P]ATP in these mutants expressed in Sf9 cells membranes showed a labeling similar to that seen for the wild-type protein, and this over a broad range of concentrations applied (5−70 μM); only a small decrease was observed in the double mutant at low 8-azido[α-^{32}P]ATP concentrations ($\leq$25 μM) (*29*). Together, these data suggest that both NB sites are essential for function, and both need to be intact for coupling drug transport to ATPase activity.

Parallel studies in the catalytic β-subunit of F_1-ATPase show that the Walker A motif lysine (K155) has direct function in nucleotide binding and catalysis. Mutations K155Q and K155E are not tolerated and exhibit less than 0.1% of the wild-type ATPase activity, probably due to loss of the positive charge providing significant binding energy (*30*). From the X-ray structure (*31*) and mutational analysis, it was concluded that the side chain of βK155 lies very close to the γ-phosphate of ATP and makes one or more specific hydrogen bonds with the γ-phosphate. Another key catalytic residue is the aspartate within the Walker B motif: structural data and biochemical studies in mutants, including nucleotide-binding studies in the presence or absence of Mg^{2+}, indicate that βD242 is involved in binding Mg^{2+} of the MgATP complex (*32, 33*). Conceptual models of ATP hydrolysis by Pgp suggest that after the initial binding of MgATP {Pgp·MgATP}, hydrolysis produces a transition state intermediate {Pgp·MgADP·P_i}, and relaxation of this high-energy state is probably coupled to drug movement (reviewed in *34*). Vanadate can interrupt the cycle by forming a stable {Pgp·MgADP·V_i} complex, which is only slowly released and which can be monitored by the appearance of trapped nucleotide (*35, 36*). Such a complex has recently been elucidated in the three-dimensional structure of myosin, and is believed to be a stable analogue of the {myosin·MgADP·P_i} transition state complex representing the status during hydrolysis (*37*). In the case of Pgp, vanadate trapping of 8-azido[α-^{32}P]ATP was shown to occur in both N- and C-terminal NB sites in a nonselective fashion, establishing that both sites are catalytically active (*35, 36*). These studies suggested (1) that only one site can be in the transition state at any given time and (2) that the two sites possibly alternate in catalysis (reviewed in *34*).

We have recently described a procedure for high-level expression of the mouse Mdr3 Pgp in the methanotropic yeast *Pichia pastoris*. In this system, the *mdr3* cDNA is inserted by homologous recombination at the *P. pastoris AOX1* chromosomal locus, a gene which can be induced at high level when methanol is provided as a sole source of carbon. In plasma membrane preparations from such induced cells, Mdr3 can account for as much as 5−10% of total membrane proteins, and Mdr3-specific drug-stimulated ATPase activity can readily be detected after simple solubilization and reconstitution steps (*38, 39*). Here, we have investigated the role of the two NB sites of Pgp in ATP hydrolysis in general, and in the catalytic cycle of the enzyme in particular. Single point mutations were introduced in the core consensus Walker A motif (K429R, K1072R, K429R/K1072R) or Walker B motif (D551N, D1196N, D551N/D1196N) in each or both NB sites of Mdr3. Wild-type and mutant enzymes were expressed in *P. pastoris*, purified to homogeneity and reconstituted in *E. coli* lipids, and tested for alterations in ATP hydrolysis. In addition, we used the technique of vanadate trapping of photoactive nucleotides as a more sensitive method of monitoring ATP hydrolysis. We were interested to determine if nucleotide binding per se or hydrolysis after the initial binding step is affected in either of the mutants, and whether single mutations in only one NB site of the Mdr3 ATPase were able to allow low-level hydrolysis and/or single-site turnover in the intact nonmutant NB site.

EXPERIMENTAL PROCEDURES

mdr3 cDNA Modifications and Plasmid Constructions. A 2.2-kb *Eco*RI fragment of *mdr3* (positions 93−2248) was cloned in the corresponding site of phage vector M13mp18, and single-stranded DNA was used as a template for site-directed mutagenesis in NBD1, using a commercially available kit (Amersham, Arlington Heights, IL). This template contains engineered *Nru*I (position 1346) and *Sal*I sites (position 1908) to facilitate subsequent cloning of the mutated cDNA portion (*40*). An existing *Bgl*II site (position 1363) was removed using oligonucleotide (5′)-CCCTTCAA**T**ATCT-GAACT-(3′) for diagnostic purposes. Mutagenic oligonucleotides for the K429R and D551N mutations were 5′-GTTGTGCTT**C**TTCCACAG-3′ and 5′GTGGCCTC**A**T**T**C-AACAAAAGG-3′, respectively. For the K1072R mutation, a 1.7-kb *Sma*I−*Pst*I *mdr3* fragment (positions 1764−3511) in M13mp19 containing unique *Nru*I (position 2724), *Sal*I (position 2480), and *Spe*I sites (position 2914) was used as template (*41*) with the mutagenic oligonucleotide 5′-TGT-GCTC**C**TCCCGCAGCC-3′. For the D1196N mutation, a *Pst*I−*Hin*dIII *mdr3* fragment (positions 3511−4199) from pDR1.6 (*42*) was inserted in the corresponding sites of M13 mp18, and a *Sna*BI site was introduced after the last amino acid (position 3889), using oligonucleotide 5′-GGTCA-CAGTTCA**TACGTA**TGAGCGCTTTGC-3′. The D1196N mutation was introduced in this template using the mutagenic oligo 5′-GATGTTGCTTCGTCGT**TT**A**A**AAGTAAAAT-GTGAG-3′. The nucleotide sequence of the mutated segments was verified prior to their insertion in the corresponding sites of pVT-*mdr3* (NBD1 mutations, *40*) or pVT-*mdr3.5* (NBD2 mutations) for biological testing in *S. cerevisiae*.

To allow direct subcloning of NBD2 fragments into the yeast expression vector pVT101-U (*43*), a 665-bp *Eco*RI−*Nru*I fragment containing the f1 origin (positions 2630−3295) was deleted from pVT101-U by restriction digest, repaired with T4 DNA polymerase, and recircularized. A series of six histidine residues were inserted in-frame at the C-terminus of the protein in a three-part ligation involving

(1) the *Pst*I−*Sna*BI *mdr3* fragment (positions 3511−4199), (2) a linker composed of two complementary oligos 5′-GTACATCACCATCACCATCACTGAACCGGT-3′ coding for a hexahistidine tail followed by a STOP codon, and an *Age*I site, and (3) the *Acc*65I−*Pst*I *mdr3* fragment (positions 93−3511). The extremities were repaired with T4 DNA polymerase followed by cloning into the *Pvu*II−*Bam*HI polylinker sites of pVT101-U to create pVT-*mdr3.5*. In this construct the *Eco*RI, *Nru*I, *Sal*I, *Spe*I, and *Age*I sites of *mdr3* are unique. The biological activity of pVT-*mdr3.5* with respect to capacity to convey cellular resistance to the fungicidal compound FK506 (50 μg/mL) was tested in the yeast *S. cerevisiae* strain JPY201, as previously described (*44*); it was found to be similar to that observed with a pVT101 construct containing wild-type *mdr3*. Expression of wild-type and mutant Pgp variants in *S. cerevisiae* membranes was monitored by Western blot analysis of crude plasma membrane preparations, using the monoclonal anti-Pgp antibody C219 (Signet Labs Inc.).

Plasmid Constructions and Transformation in Pichia pastoris. For expression and purification of wild-type Mdr3, the full-length mouse *mdr3* cDNA tagged with the C-terminal hexahistidine tail was excised from pVT-*mdr3.5* as a *Kpn*I−*Age*I fragment, and the extremities were repaired with T4 DNA polymerase prior to cloning into the *Eco*RI site of the pHIL-D2 expression vector (InVitrogen, license number 145 457) to create pHIL-*mdr3.5*−His_6. NBD1 mutants were subloned from pVT-*mdr3* as *Afl*II−*Eco*RI fragments, and NBD2 mutants were sucloned from pVT-*mdr3.5* as *Eco*RI−*Sna*BI fragments. The presence of the individual or double mutants was confirmed by sequencing. pHIL-*mdr3.5*−His_6 carrying either wild-type or mutant versions of *mdr3*, as well as the control pHIL-D2 vector, was transformed into *P. pastoris* strain GS115 according to the manufacturer instructions, using a lithium chloride technique. His^+ transformants showing successful homologous recombination at the *AOX1* locus were identified as unable to grow on medium containing methanol (methanol utilizing slow or mut^s), as we have previously described (*38*). While the expression level of Mdr3 is about 10-fold higher in *P. pastoria* than in *S. cerevisiae* (data not shown), expression under the control of the strong AOX1 promotor is only induced in methanol containing medium which slows down the growth of the yeast cultures (mut^S) and renders them unsuitable for drug resistance assays *(66)*.

Membrane Preparations. The initial screen for *P. pastoris* clones expressing P-glycoprotein (Pgp) was done on 10 mL cultures following a 48 h induction of *AOX1* with methanol, as previously described (*39*). Cells were washed with 1 mL of lysis buffer (50 mM Tris-HCl, pH 7.4, 0.33 M sucrose, 1 mM EDTA, 1 mM EGTA, 1 mM DTT) and resuspended in 300 μL of lysis buffer supplemented with protease inhibitors (10 μg/mL leupeptin, 10 μg/mL pepstatin A, and 1 mM PMSF). Cells were disrupted with a 100 μL volume of acid-washed glass beads by vortexing 4 times for 1 min, with intervening 2 min incubations on ice. Unlysed cells were removed by centrifugation for 5 min at 12000*g*, and crude plasma membranes were precipitated with 10 mM $MgCl_2$ for 15 min on ice and recovered by centrifugation (12000*g*, 20 min) (*45*). The final membrane pellet was resuspended in 25 μL of lysis buffer, and protein concentration was determined using a Bradford protein assay (BioRad). Pgp expression was monitored by immunoblotting with the anti-Pgp monoclonal antibody C219. Over 90% of the His^+mut^s transformants identified were found to express Pgp. Expression levels of wild-type and mutant Mdr3 variants in these clones (modified by addition of the hexahistidine tails) were similar, and comparable to the expression levels noted for wild-type, unmodified Mdr3 (*38*). For large-scale preparations of *P. pastoris* membranes, cultures were induced in methanol-containing medium, and plasma membranes were isolated by centrifugation on discontinuous sucrose density gradients, as previously described (*38*). From a 1 L culture, we routinely obtained 10 mg of membrane protein at the 16−31% sucrose gradient interface and about 20 mg at the 31−43% interface. A similar distribution of Pgp in two different sucrose gradient interfaces has been previously found for membrane preparations of hamster Pgp from mammalian cells (*22*). Both membrane fractions were used for further purification of Pgp.

Solubilization and Purification of P-glycoprotein. Typically, 5 mg of membranes (2 mg/mL) was first precipitated with 10 mM $MgCl_2$ (15 min, 0 °C) and recovered by centrifugation (16000*g*, 20 min) to remove EDTA, EGTA, and DTT from the preparation. Membrane pellets were resuspended in buffer A (50 mM Tris-HCl, pH 8.0, 20% glycerol, 50 mM NaCl, 5 mM imidazole, 1 mM β-mercaptoethanol) and solubilized by adding an equal volume of 1% L-α-lysophosphatidylcholine (L-PC, from egg yolk, 99% pure, Sigma) in buffer A at a protein concentration of 2 mg/mL followed by gently vortexing at 20 °C. Once solubilized, samples were chilled on ice and centrifuged at 100000*g* for 45 min to remove particulate material. The supernatant was recovered and mixed with 200 μL of Ni−NTA resin (Qiagen), equilibrated in buffer A, followed by incubation at 4 °C for 4−16 h on a Labquack rotator. The resin with the bound protein was transferred into a column and washed extensively with 6 mL (40 bed volumes) of buffer A containing 0.1% *n*-dodecyl β-D-maltoside (DM) followed by 1 mL of buffer B (50 mM Tris-HCl, pH 8.0, 20% glycerol, 40 mM NaCl, 20 mM imidazole, 0.1% DM). Pgp was then eluted with 2 mL of buffer C (50 mM Tris-HCl, pH 8.0, 20% glycerol, 80 mM imidazole, 0.1% DM) at a flow rate of 0.1 mL/min. All steps were performed at 4 °C, and the protease inhibitors 10 μg/mL leupeptin, 10 μg/mL pepstatin A, and 1 mM PMSF were added fresh to all buffers. For reconstitution of Pgp, the 80 mM imidazole eluate was incubated with 1% *Escherichia coli* lipids (Avanti, acetone/ether preparation) for 30 min on ice, followed by dialysis against 20 volumes of 50 mM Tris-HCl, pH 7.4, 0.1 mM EGTA, and 1 mM DTT. Omission of DTT resulted in a completely inactive Pgp ATPase. Pgp proteoliposomes were aliquoted and stored at −80 °C until use.

Assay of ATPase Activity. Reactions were carried out in 50 μL of 50 mM Tris-HCl, pH 8.0, 0.1 mM EGTA, 10 mM Na_2ATP, and 10 mM $MgCl_2$ at 37 °C for appropriate times during which the reaction was linear, and ≤10% of added nucleotide was hydrolyzed. Reactions were initiated by addition of purified reconstituted Pgp, and stopped by addition of 1 mL of 20 mM ice-cold H_2SO_4. P_i release was assayed by the method of (*46*). For determination of kinetic parameters, an excess of 2 mM $MgCl_2$ over MgATP concentrations was used. Drugs were added as dimethyl

sulfoxide solutions, and the final solvent concentration in the assay kept ≤2% (v/v).

Vanadate Trapping and Photoaffinity Labeling with 8-Azido-[α-^{32}P]ATP. For 8-azido[α-^{32}P]ATP photoaffinity labeling experiments, purified Pgp was reconstituted into *E. coli* lipids by dialysis in DTT-containing buffers first, followed by dialysis against 100 volumes of 20 mM Tris-HCl, pH 8.0, 0.1 mM EGTA which had been degassed and saturated with argon. DTT-free Pgp proteoliposomes were kept under an atmosphere of argon. Proteoliposomes containing wild-type or mutant Mdr3 variants were incubated with 80 μM 8-azido-[α-^{32}P]ATP (8.5 Ci/mmol), 3 mM $MgCl_2$, 200 μM vanadate, 100 μM verapamil, 20 mM Tris-HCl, pH 8.0, 0.1 mM EGTA in a total volume of 50 μL at 37 °C for the indicated times. The incubations were started by addition of Pgp and stopped by transfer on ice. Free label was promptly removed by centrifugation at 200000*g* for 30 min at 4 °C in a TL-100 rotor (Beckman), and proteoliposomes were washed and resuspended in 50 μL of ice-cold 20 mM Tris-HCl, pH 8.0, 0.1 mM EGTA. Samples were kept on ice and irradiated with UV light for 5 min (UVS-II Minerallight 260 nm placed directly above the samples). At concentrations of 80 μM 8-azido[α-^{32}P]ATP, vanadate previously induced trapping of nucleotide at a stoichiometry of 1 mol/mol of Pgp, 26% of which became covalently attached to hamster Pgp on UV irradiation and survived gel electrophoresis (*35*). A direct assessment of the trapping stoichiometry in Mdr3 proteoliposomes was not possible, because the centrifuge column technique cannot be used with proteoliposomes (*36*). To remove unbound ligands, we adapted a simple centrifugation protocol. Counting revealed that about 95% of the applied 8-azido[α-^{32}P]nucleotide was removed after centrifugation and subsequent washing. Similar results were obtained with negative control proteoliposomes purified from *P. pastoris* cells transformed with the empty pHIL-D2 plasmid. After gel electrophoresis, up to 10% of the mouse Mdr3 molecules remained covalently labeled by 8-azido[α-^{32}P]nucleotide, but no radioactivity was detected in lanes loaded with negative control proteoliposomes. Orthovanadate solutions (100 mM) were prepared from Na_3VO_4 (Fisher Scientific) at pH 10 as described (*47*) and boiled for 2 min before each use to break down polymeric species.

Routine Procedures. Protein concentrations were determined by the bicinchoninic acid method (Pierce) in the presence of 1% SDS using bovine serum albumin as a standard. SDS−PAGE was according to Laemmli (*48*) using the Mini-PROTEAN II gel and Electrotransfer system (BioRad). Samples were dissolved in 5% (w/v) SDS, 25% (v/v) glycerol, 0.125 M Tris-HCl, pH 6.8, 40 mM DTT, 0.01% pyronin Y for 30 min at 37 °C, and separated on 7.5% polyacrylamide gels. For immunodetection of Pgp, the mouse monoclonal antibody C219 (Signet laboratories Inc.) was used with the ECL detection system (Amersham). For autoradiography, SDS gels were stained with Coomassie Blue, dried, and exposed overnight at −80 °C to Kodak BioMax films with intensifying screens.

Materials. 8-Azido[α-^{32}P]ATP (8.5 Ci/mmol) and verapamil were purchased from ICN, valinomycin from Calbiochem. Acetone/ether-precipitated *E. coli* lipids were from Avanti Polar Lipids, and general chemicals were of reagent grade from Sigma.

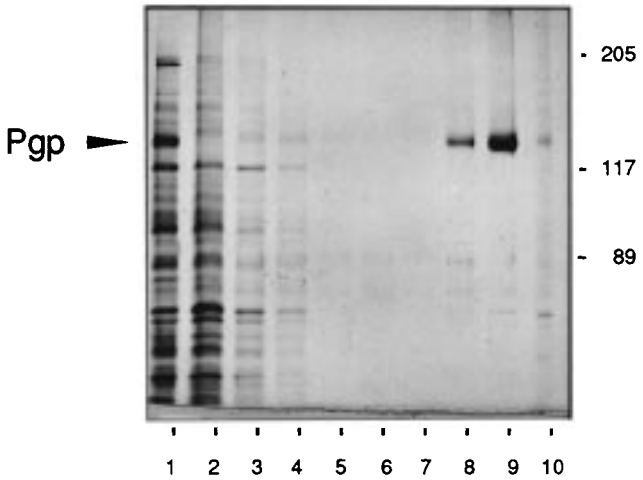

FIGURE 1: Purification of Mdr3. Plasma membranes from *P. pastoris* yeast cells expressing the Mdr3-His_6 protein (lane 1, 10 μg) were solubilized in 0.5% lysophosphatidylcholine and purified on Ni−NTA resin as described under Experimental Procedures. Samples from each step were separated on 7.5% SDS gels and stained with Coomassie Blue. Lane 2, pool of flowthrough material (10 μg); lanes 3−7, consecutive washes with 1 mL of 5 mM imidazole buffer; lane 8, 1 mL wash with 20 mM imidazole buffer; lane 9, 80 mM imidazole eluate (5 μg); lane 10, 10% SDS wash. In lanes 3−8, the entire 1 mL fractions were precipitated with 5% TCA before loading on gel. The position of molecular mass markers is given in kDa on the right.

RESULTS

Purification of P-glycoprotein (Mdr3) from P. pastoris. We added six consecutive histidine residues in-frame at the C-terminus of the mouse Mdr3 Pgp (Mdr3-His_6) and have expressed this protein in the yeast *P. pastoris* for large-scale production and purification. In individual *P. pastoris* clones transformed with pHIL-*mdr3*−His_6 constructs, the expression level of mouse Mdr3-His_6 accounted for about 5% of total plasma membrane proteins (Figure 1, lane 1). To ensure functional integrity, we monitored the ATPase activity of the Mdr3-His_6 protein from plasma membrane preparations after differential detergent extraction and reconstitution in *E. coli* lipids. The ATPase activity of Mdr3-His_6 from such plasma membrane preparations was indistinguishable from that of wild-type Mdr3 prepared in a similar fashion (*38*), with respect to K_M, V_{max}, and drug stimulation profiles (data not shown). Subsequently, Mdr3-His_6 was extracted from the membrane with L-α-lysophosphatidylcholine (L-PC, 0.5% w/v) for purification on Ni−NTA resin (Figure 1). In initial pilot experiments, we noted that a 4−16 h incubation (at 4 °C) of the detergent extract with the Ni−NTA resin was required for optimal Mdr3 binding to the resin, with minimal amounts remaining in the flow-through from the column (lane 2). The Ni−NTA resin was then washed extensively with low concentrations of imidazole (5 and 20 mM, 50 bed volumes, lanes 3−8) to remove possible contaminants. Finally, Mdr3-His_6 could be efficiently eluted from the column with 80 mM imidazole (lane 9), with little if any Mdr3-His_6 remaining associated to the Ni−NTA resin (lane 10). As seen in Figure 1 (lane 9), the Mdr3-His_6 protein could be recovered in almost pure form by this procedure, and 20−30 μg of purified Mdr3-His_6 could be routinely obtained from 5 mg of plasma membranes of *P. pastoris* cells.

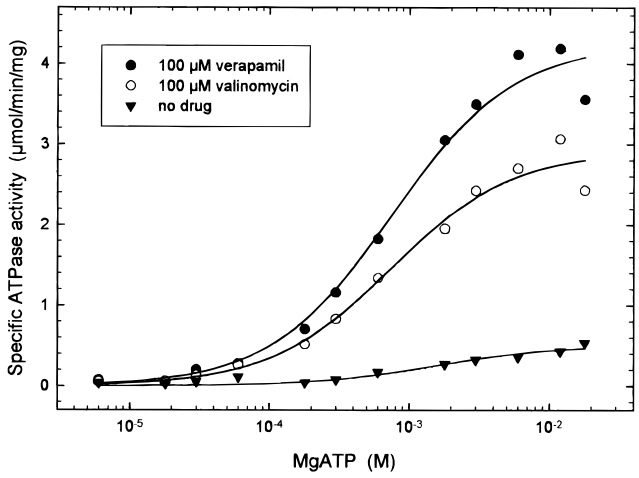

FIGURE 2: Specific ATPase activity of purified reconstituted Mdr3. The specific ATPase activity of purified reconstituted Mdr3 was measured as a function of MgATP concentrations in the absence or presence of 100 μM verapamil or 100 μM valinomycin. The maximum velocity in the presence of verapamil was 4.3 μmol min^{-1} mg^{-1}, in the presence of valinomycin 2.9 μmol min^{-1} mg^{-1}, and in the absence of drug 0.5 μmol min^{-1} mg^{-1}. The curves are nonlinear least-squares regression fits of the data points to the Michaelis−Menten equation.

ATPase Activity. Pgp-specific and verapamil-stimulated ATPase activity was readily detectable after reconstitution of the purified Mdr3-His$_6$ into *E. coli* lipids. Maximal stimulation was seen at 100 μM verapamil, and the ATPase activity ranged from 3 to 4.3 μmol min^{-1} mg^{-1} in different preparations of purified protein (k_{cat} 7−10 s^{-1}) (Figure 2). Valinomycin also induced robust stimulation of the ATPase activity of Mdr3-His$_6$ (Figure 2). In the absence of drugs, the specific ATPase activity was very low, between 0.35 and 0.65 μmol min^{-1} mg^{-1}. The high degree of drug-stimulatable ATPase activity above background observed here (8-fold for verapamil, 6-fold for valinomycin) and previously (*21*, *24*) might be linked to the absence of lipids during chromatography: possibly, extensive washes with detergent-containing buffers result in the removal of tightly associated lipids, which might (themselves) be endogenous transport substrates for the Pgp ATPase (*6*, *7*). Nevertheless, the maximum drug-stimulated ATPase activity of the purified reconstituted Mdr3-His$_6$ protein was found to be very similar to that of other Pgp preparations purified from mammalian cells (*22*, *23*, *26*). This indicates that the Mdr3-His$_6$ purified from *P. pastoris* is fully functional, and that the hexahistidine tag does not affect function. Inclusion of high NaCl concentrations (400−500 mM) in the solubilization and chromatography buffers, as used for purification of a His-tagged human MDR1 (*24*, *25*), was deleterious and resulted in very low Mdr3 ATPase activity after reconstitution (data not shown). Therefore, the NaCl concentration in our purification scheme was kept at 50 mM in the initial solubilization and wash buffers, and further reduced as the imidazole concentration was increased (Experimental Procedures).

Purified reconstituted Mdr3 showed a single, high K_M for MgATP hydrolysis (Figure 2) which was similar in the absence (0.9 mM) or presence of verapamil (0.75 mM) or valinomycin (0.74 mM), indicative of low-affinity nucleotide-binding sites in Mdr3, similar to hamster Pgp1 and human MDR1 (*5*, *17*, *49*). The verapamil-stimulated ATPase activity was completely inhibited by 200 μM vanadate with half-maximal inhibition occurring around 5 μM; 10 mM sodium-azide, an inhibitor of the mitochondrial F_1-ATPase, did not affect the purified reconstituted Mdr3 ATPase. No Ca^{2+}-ATPase activity was detected when assayed in the absence or presence of 2 mM EGTA. Mg-8-azido-ATP was also a substrate for the purified reconstituted Mdr3 ATPase and was hydrolyzed with a specific activity of 1.5 μmol min^{-1} mg^{-1} in the presence of 100 μM verapamil. At 80 μM 8-azido-ATP, as used during photolabeling and vanadate trapping experiments (see later), it was estimated that Mdr3 hydrolyzed one molecule of 8-azido-ATP every 3 s. Finally, we purified the same amount of plasma membranes from control *P. pastoris* cells transformed with the empty pHIL-D2 vector and reconstituted the 80 mM imidazole fraction. The same volume equivalent of these control proteoliposomes showed less than 5% ATPase activity of Mdr3 proteoliposomes. This low level of ATPase activity was not stimulatable by verapamil and was probably due to very low levels of contaminating yeast plasma membrane H^+-ATPase (PMA1) which is abundant in the starting material.

Effects of NB Site Mutations on Mdr3 Function. Pgp contains two nucleotide-binding sites with consensus sequence motifs known as Walker A (GNSGCG**K**S and GSSGCG**K**S) and Walker B motifs (ILLL**D** in both sites) which are present in every member of the ABC family. Single-point mutations K429R and K1072R were introduced in the Walker A motif at each NB site, and single mutations D551N and D1196N were introduced independently in the Walker B motif of each NB site. Mutations were inserted in pVT-*mdr3* and transformed in the yeast *Saccharomyces cerevisiae*. Immunoblotting of crude membrane fractions from yeast transformants expressing individual mutants using the anti-Pgp antibody C219 showed similar levels of expression of the various Pgp mutants (Figure 3, inset). This indicates that mutations in the NB sites do not have a major effect on protein stability or membrane targeting in yeast. To assess the biological activity of these mutants, their ability to confer resistance to the fungicide FK506 was tested in a growth inhibition assay in liquid medium previously developed in our lab (*40*, *41*, *44*). As shown in Figure 3, cells expressing wild-type Mdr3 grew well in FK506-containing medium while all single-point mutants failed to grow, and as such were indistinguishable from negative control *S. cerevisiae* cells transformed with the empty pVT vector. These results are consistent with earlier reports on mouse Mdr1 and human MDR1 expressed in mammalian cells, and indicate that mutations in the Walker A (*27*, *28*) and Walker B motifs (this study) abrogate the capacity of Pgp to confer drug resistance.

Expression and Purification of NB Site Mutants in Pichia pastoris. For large-scale production of plasma membranes and subsequent Mdr3 purification, we reconstructed the K429R, K1072R (Walker A) and D551N, D1196N (Walker B) single mutants and the K429R/K1072R, D551N/D1196N double mutants in plasmid vector pHIL-*mdr3*−His$_6$ and expressed the corresponding Pgp variants in the yeast *Pichia pastoris*. Crude membrane fractions were prepared from independent colonies of *P. pastoris* transformants and analyzed for Mdr3 protein expression. All Mdr3 mutants could be stably expressed in membrane fractions of *P. pastoris*, and the levels of expression of the mutants were

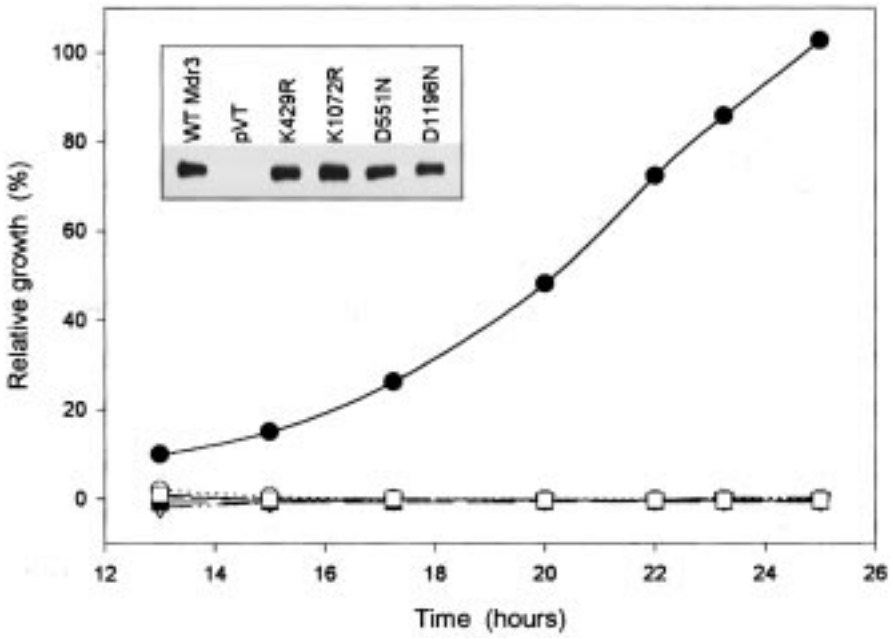

FIGURE 3: Biological activity of wild-type and mutant Mdr3 variants. The capacity of Mdr3 to confer cellular resistance to the fungicide FK506 in the yeast *Saccharomyces cerevisiae* was measured for wild-type Mdr3 (wild-type, ●) and mutants K429R (▼), K1072R (▽), and D551N (■), D1196N (□), and for control pVT vector (○) transformants. Growth of individual mass populations in 50 μg/mL FK506 is expressed as the relative growth compared to growth of the same cell populations in drug-free medium (expressed as a percentage). Insert: Western blot analysis of crude plasma membranes from individual mass populations with the mouse monoclonal anti-Pgp antibody C219.

very similar, and also similar to that seen in cells expressing wild-type Mdr3 (data not shown). Individual and double Mdr3 mutants were purified from large-scale plasma membrane preparations by Ni−NTA chromatography followed by reconstitution in *E. coli* lipids. All mutant proteins yielded Mdr3 in equal purity and in similar amounts, comparable to those seen for the wild-type protein, as judged by Coomassie blue stained SDS gels and Western blot analysis (Figure 4). The specific ATPase activity of the purified reconstituted Mdr3 NB sites mutants was measured and found to be very low, varying between 0.025 and 0.1 μmol^{-1} min^{-1} mg^{-1} (averages from two purifications each), a background value similar to that measured in control proteoliposomes prepared from the pHIL-D2 vector. This very low level of ATPase activity accounted for less than 5% of the Mdr3 wild-type activity, was not stimulated by verapamil, and was probably caused by low-level contamination from residual plasma membrane ATPases. These results indicate that mutations in the Walker A and B motifs of either NB site abrogate the capacity of Mdr3 to convey drug resistance, by inactivating the ATPase activity of the protein.

Photolabeling with Mg-8-azido[α-^{32}P]ATP. A comparison with other ATPases reveals that mutations of equivalent residues in the catalytic β-subunit of F_1-ATPase (K155Q, K155E and D242N, D242V) cause a dramatic reduction in ATPase activity (less than 0.1% of wild-type) which is associated with a reduction in binding affinity for MgATP by more than 2 orders of magnitude (*30*). We were therefore interested in assessing the effect of single or double mutations in Walker A and B motifs on ATP binding in general, and in particular determining if a mutation in one NB site would allow ATP binding and low-level hydrolysis at the other, nonmutant NB site. To monitor the nucleotide-binding properties of Mdr3 mutants, we used photoaffinity labeling with a nucleotide analogue. Purified reconstituted proteins were incubated with the photoaffinity analogue 8-azido[α-^{32}P]-ATP in the presence of Mg^{2+} for 5 min at RT, followed by UV-irradiation on ice. Labeled proteins were separated

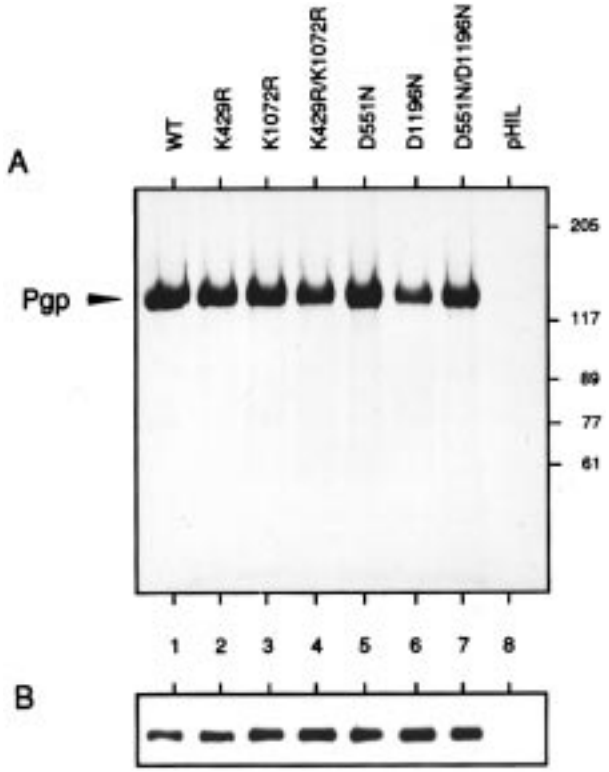

FIGURE 4: Purification of NB site mutants from *Pichia pastoris* membranes. Wild-type and mutant Mdr3-His_6 variants (identified on top of panel A) were expressed in the yeast *P. pastoris* and purified by Ni−NTA chromatography. 300 μL of the 80 mM imidazole fractions (3−5 μg of Mdr3 protein) was precipitated with TCA, subjected to SDS gel electrophoresis, and stained with Coomassie Blue (A) or analyzed by Western blot using the mouse monoclonal anti-P-glycoprotein antibody C219 (B). The position of molecular mass markers is given in kDa on the right.

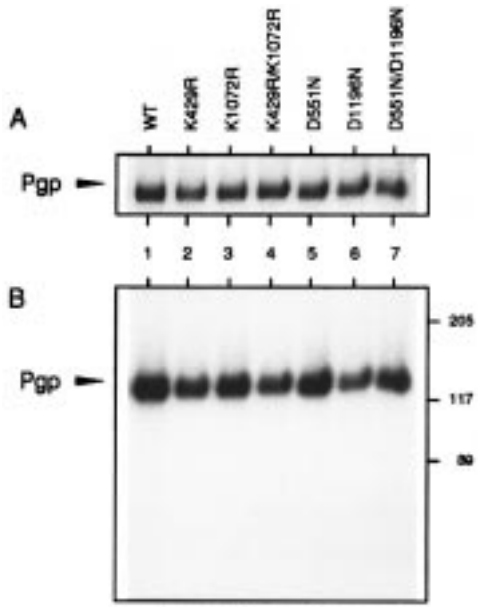

FIGURE 5: Direct photolabeling of purified reconstituted Mdr3 NB site mutants. Three micrograms of purified reconstituted wild-type and mutant Mdr3 variants was UV-irradiated in the presence of 80 μM 8-azido[α-^{32}P]ATP and 3 mM $MgCl_2$. Photolabeled samples were separated on 7.5% SDS gels and stained with Coomassie Blue (A) followed by autoradiography (B). The position of molecular mass markers is given on the right.

on SDS gels, stained with Coomassie Blue, and subjected to autoradiography (Figure 5). Binding and subsequent photo-cross-linking of the radionucleotide was specific to Mdr3 which is the major protein (≥90% pure) in our preparations. The amount of ^{32}P label incorporated in each mutant was found to be very similar to that incorporated in the wild-type Mdr3 protein. In these experiments, we used 80 μM 8-azido[α-^{32}P]ATP, a suboptimal concentration 10 times lower than the K_M value for 8-azido-ATP hydrolysis (0.8 mM, *22*). Therefore, these results suggest that none of the introduced single or double mutations affected significantly the nucleotide-binding properties of Mdr3. This is consistent with the notion that the key catalytic residues K429, K1072 and D551, D1196 in the Walker A and Walker B motifs participate mostly in the hydrolysis steps after the initial binding of ATP.

Vanadate Trapping with Mg-8-azido[α-^{32}P]ATP. We used the technique of vanadate trapping of nucleotide to monitor hydrolysis of Mg-8-azido[α-^{32}P]ATP in each of the NB site mutants of Mdr3. It has been previously established that vanadate trapping requires hydrolysis of ATP and that the trapped nucleotide species in Pgp is ADP (*35*, *36*, *50*). In initial experiments, we preincubated wild-type and mutant Mdr3 variants for 1−10 min at 22 °C with Mg-8-azido[α-^{32}P]ATP in the presence of vanadate to allow trapping; unbound ligands were removed by centrifugation, and UV irradiation was used to cross-link the trapped nucleotide. Photolabeling of the radionucleotide was readily detectable in the wild-type Mdr3 protein after only 1 min of trapping, and this labeling saturated rapidly upon increasing the trapping periods. However, nucleotide trapping under these conditions was completely abolished in all of the single- and double-point mutations of the Walker A motif (shown in Figure 6A) and Walker B motif (data not shown). To obtain an estimate of the loss of activity in the mutant proteins, we examined the time dependence of vanadate trapping of nucleotide in wild-type Mdr3. As shown in Figure 7, vanadate could trap visible amounts of 8-azido[α-^{32}P]-nucleotide in wild-type Mdr3 within a short incubation period of 10 s. However, increasing the trapping periods for up to 60 min at 37 °C failed to produce any detectable vanadate-induced trapping and photolabeling of Mg-8-azido[α-^{32}P]-ADP in the mutant proteins, and were indistinguishable from control samples preincubated in the absence of vanadate (Figure 6B,C). From this, we conclude that all NB site mutants hydrolyze at least 360 times slower than the wild-type protein (<0.3% activity). Interestingly, not even the single-point mutants were able to trap visible amounts of radionucleotide regardless of the location of the mutation in the first or second NB site. These results indicate that while all NB site mutants can bind the Mg-8-azido[α-^{32}P]ATP probe with wild-type characteristics (Figure 5), vanadate cannot induce trapping of Mg-8-azido[α-^{32}P]ATP in any of these mutants. Since the trapped species is known to be ADP, the mutants appear totally defective in ATP hydrolysis, suggesting that both NB sites need to be intact for even a single turnover event in the full-length protein.

DISCUSSION

The yeast *P. pastoris* offers an economical alternative to the large-scale production and isolation in pure form of P-glycoprotein (Mdr3) by a standard affinity purification protocol. The purified Mdr3 reconstituted in *E. coli* lipids exhibits high verapamil and valinomycin-stimulated ATPase activity with a maximal velocity of 4.3 μmol min^{-1} mg^{-1}, an 8-fold stimulation over basal Mdr3 ATPase activity (0.5 μmol min^{-1} mg^{-1}). The catalytic properties of this Mdr3 preparation were very similar to those previously published for Pgp purified from mammalian and insect cells; e.g., the K_M for MgATP was 0.8 mM and the K_i for vanadate 5 μM, indicating that Mdr3 purified from *P. pastoris* plasma membranes is highly functional. Single-point mutations introduced into the core consensus sequences of the Walker A motif (K429R, K1072R) or the Walker B motif (D551N, D1196N) in either of the two nucleotide-binding (NB) sites impaired the capacity of Mdr3 to confer cellular resistance to the fungicide FK506 in the yeast *Saccharomyces cerevisiae*, indicating that these residues are critical for function. Mutations K429R, K1072R and D551N, D1196N as well as the double mutations K429R/K1072R (Walker A motif) and D551N/D1196N (Walker B motif) all severely decreased ATPase activity to very low levels (<5%). This low ATPase activity was not stimulated by verapamil or valinomycin, and was similar to that seen in control proteoliposomes prepared from membranes of control *P. pastoris* transformants (pHIL-D2). The data are consistent with previous mutagenic analyses of P-glycoprotein, which showed that mutations in either or both Walker A motifs rendered the protein nonfunctional in mammalian cells, with respect to cellular resistance to adriamycin and colchicine, and transport of [^{3}H]-vinblastine (*27*, *28*). Likewise, these results are in agreement with those of Loo and Clarke (*24*), who reported loss of basal and drug-stimulated ATPase activity in purified human MDR1 bearing mutations at the core GK residues in the Walker A motif.

In this study, we further investigated the mechanistic basis for the loss of function observed in the Walker A and Walker

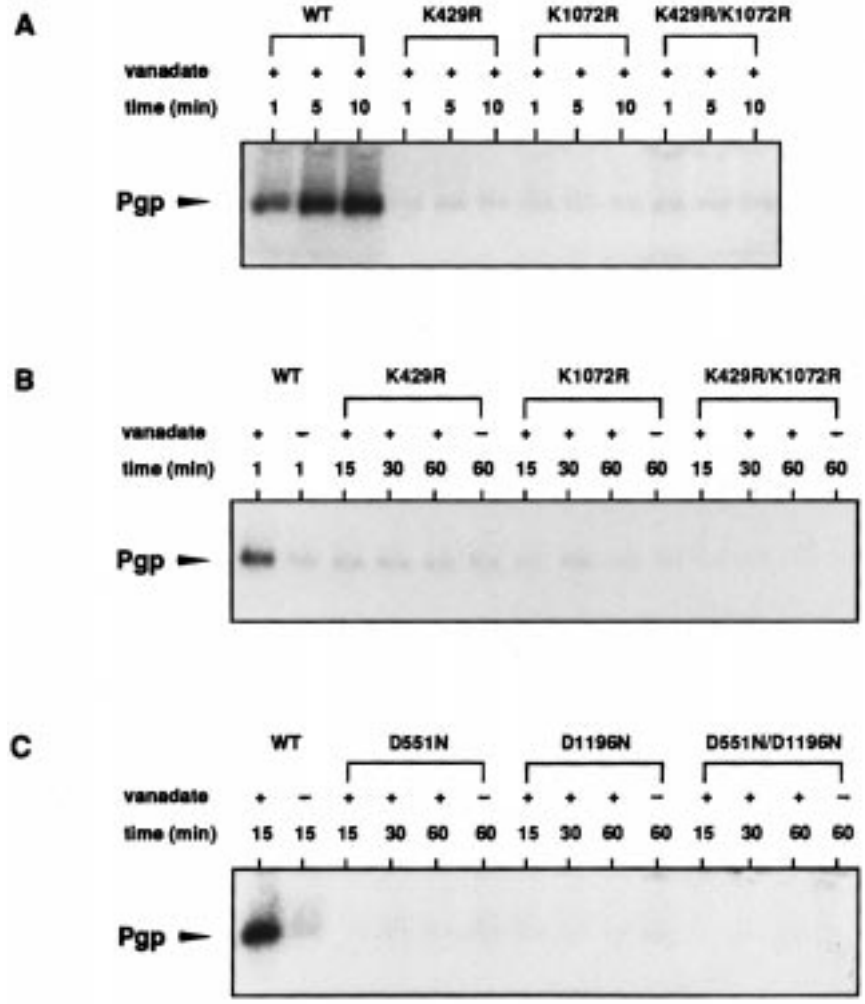

FIGURE 6: Photolabeling of Mdr3 NB site mutants by vanadate trapping with Mg-8-azido[α-^{32}P]ATP. Purified reconstituted wild-type and mutant Mdr3 variants were preincubated with 80 μM 8-azido[α-^{32}P]ATP, 3 mM $MgCl_2$, and 100 μM verapamil in the absence or presence of 200 μM vanadate at 37 °C. Unbound ligands were removed by ultracentrifugation and washing followed by UV-irradiation (Experimental Procedures). Photolabeled samples were separated by electrophoresis on SDS gels and subjected to autoradiography. The times of preincubation at RT (A) or 37 °C (B and C) are shown above the lanes. Experiments were done in duplicate.

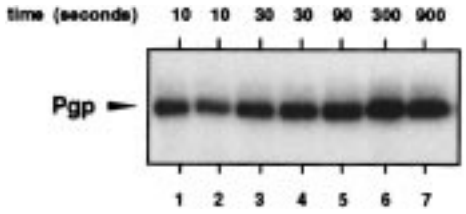

FIGURE 7: Time dependence of vanadate trapping of Mg-8-azido-[α-^{32}P]ATP in wild-type Mdr3. Experiments were performed as in Figure 6 in the presence of 200 μM vanadate; the times of preincubation at 37 °C are shown above the lanes.

B mutants of Mdr3. We applied the technique of vanadate trapping of nucleotide as a sensitive method to monitor Mdr3 specific ATP hydrolysis in purified reconstituted NB mutants. Previous studies have shown that (a) vanadate in the presence of Mg-8-azido[α-^{32}P]ATP can induce trapping of the 8-azido-[α-^{32}P]nucleotide in the catalytic sites of Pgp, (b) trapping required hydrolysis of 8-azido-ATP to 8-azido-ADP, (c) formation of a stable {Pgp**·Mg·8-azido-ADP·V_i} transition state complex allowed removal of unbound ligands, and (d) subsequent photoirradiation of the isolated complex demonstrated bound 8-azido[α-^{32}P]nucleotide in both nucleotide-binding sites of Pgp (*35, 36, 50*). Therefore, this method seemed suitable for measuring Mdr3-specific single-site turnover in NB site mutants. However, we could not detect vanadate-specific trapping and photolabeling with Mg-8-azido[α-^{32}P]ATP in any of the mutant enzymes, even after an extended 60 min trapping period at 37 °C (Figure 6). At concentrations of 80 μM Mg-8-azido[α-^{32}P]ATP used in the trapping experiments, binding of nucleotide was not significantly impaired in the mutant enzymes as shown by direct photolabeling in Figure 5. The data suggest that binding per se is not the major cause of dysfunction, but steps after initial binding and involved in the hydrolysis of ATP are impaired, confirming that K429, K1072 and D551, D1196, respectively, are key catalytic residues in Mdr3.

Based on the previous example of the dynein ATPase (*51*), we speculated that the first catalytic turnover may rapidly produce a Mg·ADP intermediate that favors binding of vanadate; in this scenario, formation of the vanadate-trapped Pgp**·MgADP·V_i complex would be rapid and therefore detectable in photolabeling experiments. Indeed, we detected photolabeling in the wild-type Mdr3 protein with Mg-8-azido[α-^{32}P]nucleotide within 10 s of trapping with vanadate, the shortest time point studied. Interestingly, none of the single-point mutants in either of the two NB sites could trap detectable amounts of Mg-8-azido[α-^{32}P]ADP even after a

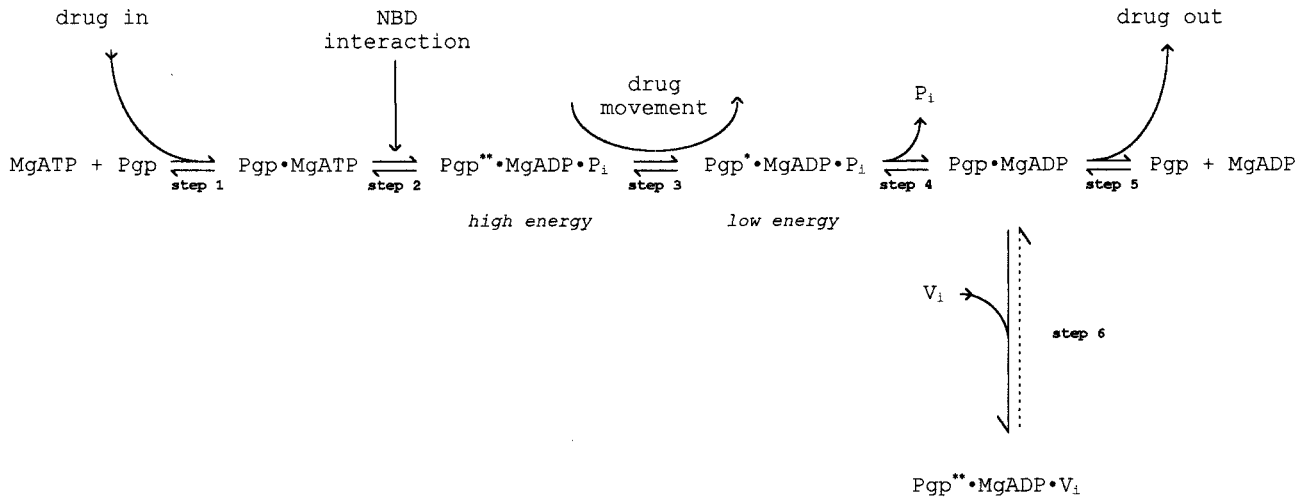

FIGURE 8: Scheme for ATP hydrolysis and vanadate-induced inhibition of P-glycoprotein. Modified from (*35*).

prolonged 60 min incubation period. The result was identical for mutations introduced either in the A or in the B motifs, in the first or second NB site, or both sites. If, as postulated, hydrolysis would simply alternate between the two NB sites, mutations in one site should allow for a single turnover in the intact site before catalysis comes to a halt (reviewed in *34*). Therefore, we might have expected in single-site mutants some trapping of nucleotide in the nonmutant NB site. The noted absence of nucleotide trapping in any of the mutants suggests that cooperative interactions may occur very early in the hydrolysis cycle, and also suggests that cooperative interactions may originate from both sites.

We propose a scheme for ATP hydrolysis and vanadate-induced inhibition in Pgp (Figure 8). This scheme draws on work presented here and previously (*34*, *35*): Hydrolysis of ATP is a multistep process initiated after binding of MgATP (step 1), by an attack of a water molecule on the γ-phosphorus to form a transition state intermediate {Pgp**•MgADP•P_i} (step 2). For simplicity, our scheme shows "drug in" at step 1 of the cycle allowing for the possibility that drugs can bind to membrane regions of the protein and ATP can bind to NB sites independently of each other, and in any order. Evidence provided from fluorescence quenching experiments with MIANS-labeled Pgp has shown that the presence of ATP is not a prerequisite for drug binding to membrane regions (*67*). On the other hand, verapamil did not affect the K_M of MgATP hydrolysis nor did it significantly alter binding of 8-azido-ATP to Mdr3 (data not shown). It appears that verapamil stimulated hydrolysis of ATP (and 8-azido-ATP) in the wild-type enzyme not by increasing the affinity of the NB sites for MgATP (step 1) but rather by accelerating the following steps with the result of an overall increased hydrolysis rate. Relaxation of the high-energy {Pgp**•MgADP•P_i} state in step 3 is then coupled to drug movement from an inside-facing segment of higher affinity to an outside-facing site of lower affinity (*52*−*54*). Finally, P_i is released from the site (step 4) followed by MgADP (step 5), and one hydrolysis cycle is completed. The next cycle will occur in the second site as postulated for an alternating catalytic sites cycle proposed by Senior et al. (*34*).

In Pgp, mutants in either NB site prevented the occurrence of the stable {Pgp**•MgADP•V_i} complex (step 6) in both sites. Formation of this complex requires hydrolysis of MgATP and release of P_i before vanadate can bind, suggesting that cooperative interactions between the two NB sites may be required for any of the steps 2, 3, 4, or 6 in the scheme to occur. We favor cooperation at step 2 because the crystal structures of other ATPases together with kinetic analysis of Walker A and B motif mutants have established that the key catalytic residues mutated in our study serve to orient and activate the γ-phosphoryl group of ATP and provide stabilization of the transition state (*30*, *55*−*57*; for a comprehensive and illustrative review, see *58*). Since verapamil and other drugs stimulated ATPase in the wild-type Mdr3 but did not do so in the NB site mutants, we propose that drug binding to the membrane regions of the protein may induce interaction of the two NB sites to provide acceleration of step 2, thus achieving the rapid turnover necessary to drive efficient drug transport.

Mutagenesis of the key residues of the Walker A and B motifs has been used to gain insight into the role of the two NB sites in catalysis and regulation of other ABC transporters. Such studies have revealed similarities and differences in the respective role of the two sites in overall function of the proteins. In the cystic fibrosis transmembrane conductance regulator (CFTR), mutations of the conserved Walker A lysine altered the conductive properties of the Cl^- channel: the K464A mutation in NB1 decreased the frequency of channel openings, whereas K1250A or K1250M in NB2 prolonged the open state of the channel (*59*). These data suggested that ATP hydrolysis at NB1 initiates opening of the channel, and hydrolysis at NB2 is required to close the channel. Nevertheless, strong cooperative interactions between the two NB sites of CFTR were suggested from a decreased rate of channel opening seen in NB2 mutants and from multiple kinetic analyses (reviewed in *60*). Multiple sequence alignments have suggested that the NB sites of CFTR might be more related to those of G-proteins, such as p21ras (*61*, *62*). The observation that the D57A mutation in a Walker B related motif of p21-H-ras retains 43% of wild-type GTPase activity (*63*) parallels the observation that NB site mutants in CFTR do support some channel gating. The ATPase activity of Walker motif mutants has been studied in another ABC protein, the *E. coli* ArsA protein. The purified ArsA mutant K21E (in NB1) showed no

significant substrate (oxyanion)-stimulated ATPase activity, while the equivalent mutation in NB2 (K340E) retained 20% of the activity. Furthermore, significant differences in the binding affinities were apparent in the NB site mutants: while K21E showed little or no photolabeling with Mg-[α-^{32}P]ATP, K340E photolabeled as well as the wild-type (*64*), suggesting structural/functional differences between the two NB sites. A similar situation seems to occur in the sulfonylurea receptor SUR1. Point mutations in the Walker A and B motifs of NB1, K719R, K719M, and D854N impaired 8-azido[α-^{32}P]ATP binding, whereas NB2 mutations, K1385R, K1385M, and D1506N, retained their ability to bind low concentrations of 8-azido[α-^{32}P]ATP in the presence or absence of Mg^{2+} (*65*). Unlike Pgp, ArsA protein and SUR1 may have one high-affinity ATP site in NB1 and a second low-affinity site in NB2.

In Pgp, however, there is no biochemical or genetic evidence to suggest that the two NB sites are functionally different (reviewed in *34*). The working model proposed in Figure 8 implies that one catalytic cycle involves hydrolysis of one MgATP and is coupled stoichiometrically to one transport event (reviewed in *60*). The question as to why Pgp and other members of the ABC family require concerted interaction of two intact NB sites for efficient ATP-energized transport and what are the structural and functional advantages of this arrangement remain to be clarified.

ACKNOWLEDGMENT

We thank Dr. Alan Senior and Dr. John Hanrahan for critical reading of the manuscript and Dr. Joachim Weber for helpful discussions.

REFERENCES

1. Goldstein, L. J. (1995) *Curr. Probl. Cancer 19*, 65−124.
2. Gottesman, M. M., and Pastan, I. (1993) *Annu. Rev. Biochem. 62*, 385−427.
3. Gros, P., and Buschman, E. (1993) *Int. Rev. Cytol. 137C*, 169−197.
4. Ruetz, S., and Gros, P. (1994) *Cell 77*, 1071−1081.
5. Shapiro, A. B., and Ling, V. (1995) *J. Bioenerg. Biomembr. 27*, 7−13.
6. Van Helvoort, A., Smith, A. J., Sprong, H., Fritzsche, I., Schinkel, A. H., Borst, P., and van Meer, G. (1996) *Cell 87*, 507−517.
7. Ruetz, S., and Gros, P. (1997) *Biochemistry 36*, 8180−8188.
8. Walker, J. E., Saraste, M., Runswick, M. J., and Gay, N. J. (1982) *EMBO J. 1*, 945−951.
9. Higgins, C. F. (1992) *Annu. Rev. Cell Biol. 8*, 67−113.
10. Loe, D., Deeley, R. G., and Cole, S. P. C. (1996) *Eur. J. Cancer 32A*, 945−957.
11. Riordan, J. R., Rommens, J. M., Kerem, B., Alon, N., Rozmahel, R., Grzelczak, Z., Zielenski, J., Lok, S., Plavsic, N., Chou, J. L., et al. (1989) *Science 245*, 1066−1073.
12. Aguilar-Bryan, L., Nichols, C. G., Wechsler, S. W., Clement, J. P., Boyd, A. E., Gonzales, G., Herrera-Sosa, H., Nguy, K., Bryan, J., and Nelson, D. A. (1995) *Science 268*, 372−373.
13. Ames, G. FL., and Mirura, C. S. (1992) *Adv. Enzymol. 65*, 1−50.
14. Van Veen, H. W., Bolhuis, H., Putman, M., and Konings, W. N. (1996) in *Handbook of Biological Physics* (Konings, W. N., Kabacj, H. R., and Lolkema, L. S., Eds.) Vol. 2, pp 165−188, Elsevier, Amsterdam.
15. German, U. A. (1996) *Eur. J. Cancer 32A*, 927−944.
16. Gros, P., and Hanna, M. (1996) in *Handbook of Biological Physics* (Konings, W. N., Kaback, H. R., and Lolkema, L. S., Eds.) Vol. 2, pp 137−163, Elsevier, Amsterdam.
17. Senior, A. E., Al-Shawi, M. K., and Urbatsch, I. L. (1995) *J. Biomembr. Bioenerg. 27*, 31−36.
18. Loo, T. W., and Clarke, D. M. (1995) *J. Biol. Chem. 270*, 22957−22961.
19. Sarkadi, B., Price, E. M., Boucher, R. C., Germann, U. A., and Scarborough, G. A. (1992) *J. Biol. Chem. 267*, 4854−4858.
20. Al-Shawi, M. K., and Senior, A. E. (1993) *J. Biol. Chem. 268*, 4197−4206.
21. Shapiro, A. B., and Ling, V. (1994) *J. Biol. Chem. 269*, 3745−3754.
22. Urbatsch, I. L., Al-Shawi, M. K., and Senior, A. E. (1994) *Biochemistry 33*, 7069−7076.
23. Sharom, F. J., Yu, X., Chu J. W. K., and Doige, C. A. (1995) *Biochem. J. 308*, 381−390.
24. Loo, T. P., and Clarke, D. M. (1995) *J. Biol. Chem. 270*, 21449−21452.
25. Mao, Q., and Scarborough, G. A. (1997) *Biochim. Biophys. Acta 1327*, 107−118.
26. Callaghan, R., Berridge, G., Ferry, D. R., and Higgins C. F. (1997) *Biochim. Biophys. Acta 1328*, 109−124.
27. Azzaria, M., Schurr, E., and Gros, P. (1989) *Mol. Cell. Biol. 9*, 5289−5297.
28. Roninson, I. B. (1992) *Biochem. Pharmacol. 43*, 95−102.
29. Müller, M., Bakos, E., Welker, E., Váradi, A., Germann, U. A., Gottesman, M. M., Morse, B. S., Roninson, I. B., and Sarkadi, B. (1996) *J. Biol. Chem. 271*, 1877−1883.
30. Senior, A. E., and Al-Shawi, M. K. (1992) *J. Biol. Chem. 267*, 21471−21478.
31. Abraham, J. P., Leslie, A. G. W., Lutter, R., and Walker, J. (1994) *Nature 340*, 621−628.
32. Weber, J., and Senior, A. (1997) *Biochim. Biophys. Acta 1319*, 19−58.
33. Weber, J., Hammond, S. T., and Senior, AE. (1998) *Biochemistry 37*, 608−614.
34. Senior, A. E., Al-Shawi, M. K., and Urbatsch, I. L. (1995) *FEBS Lett. 377*, 285−289.
35. Urbatsch, I. L., Sankaran, B., Bhagat, S., and Senior, A. E. (1995) *J. Biol. Chem. 270*, 26956−26961.
36. Urbatsch, I. L., Sankaran, B., Weber, J., and Senior, A. E. (1995) *J. Biol. Chem. 270*, 19383−19390.
37. Smith, C. A., and Rayment, I. (1996) *Biochemistry 35*, 5404−5417.
38. Beaudet, L., Urbatsch, I. L., and Gros, P. (1997) *Methods Enzymol.* (in press).
39. Beaudet, L., Urbatsch, I. L., and Gros, P. (1998) unpublished experiments.
40. Beaudet, L., and Gros, P. (1995) *J. Biol. Chem. 270*, 17159−17170.
41. Hanna, M., Brault, M., Kwan, T., Kast, C., and Gros, P. (1996) *Biochemistry 35*, 3625−3635.
42. Devault, A., and Gros, P. (1990) *Mol. Cell. Biol. 10*, 1652−1663.
43. Vernet, T., Dignard, D., and Thomas, D. Y. (1987) *Gene 52*, 225−233.
44. Raymond, M., Gros, P., Whiteway, M., and Thomas, T. Y. (1992) *Science 256*, 232−234.
45. Lin, P. H., Selinfreund, R., Wakshull, E., and Wharton, W. (1987) *Biochemistry 26*, 731−736.
46. Van Veldhoven, P. P., and Mannaerts, G. P. (1987) *Anal. Biochem. 138*, 45−48.
47. Godno, C. C. (1982) *Methods Enzymol. 85*, 116−123.
48. Laemmli, U. K. (1970) *Nature 227*, 680−683.
49. Sharom, F. J. (1995) *J. Bioenerg. Biomembr. 27*, 14−21.
50. Sankaran, B., Baghat, S., and Senior, A. E. (1997) *Arch. Biochem. Biophys. 341*, 160−169.
51. Shimizu, T., and Johnson, K. A. (1983) *J. Biol. Chem. 258*, 13833−13840.
52. Ruetz, S., and Gros, P. (1994) *J. Biol. Chem. 269*, 12277−12284.
53. Bolhuis, H., Van Veen, H. W., Molenaar, D., Poolman, B., Driessen, A. J., and Konings, W. N. (1996) *EMBO J. 15*, 4239−4245.

54. Dey, S., Ramachandra, M., Pastan, I., Gottesman, M. M., and Ambudkar, S. V. (1997) *Proc. Natl. Acad. Sci. U.S.A. 94*, 10594−10599.
55. Rehrauer, W. M., and Kowalczykowski, S. C. (1993) *J. Biol. Chem. 268*, 1292−1297.
56. Tian, G., Yan, H., Jiang, R., Kishi, F., Nakazawa, A., and Tsai, M. D. (1990) *Biochemistry 29*, 4296−4304.
57. Yan, H., and Tsai, M. D. (1991) *Biochemistry 30*, 5539−5546.
58. Mildvan, A. S. (1998) *Proteins: Struct., Funct., Genet. 29*, 401−416.
59. Carson, M. R., and Welsh, M. J. (1995) *Biophys. J. 69*, 2443−2448.
60. Senior, A. E., and Gadsby (1997) *FEBS Lett.* (in press).
61. Carson, M. R., Travis, S. M., and Welsh, M. J. (1995) *J. Biol. Chem. 270*, 1711−1717.
62. Manavalan, P., Dearborn, D. G., McPherson, J. M., and Smith, A. E. (1995) *FEBS Lett. 366*, 87−91.
63. John, J., Rensland, H., Schlichting, I., Vetter, I., Borasio, G. D., Goody, R. S., and Wittinghofer, A (1993) *J. Biol. Chem. 268*, 923−929.
64. Kaur, P., and Rosen, B. (1992) *J. Biol. Chem. 267*, 19272−19277.
65. Ueda, K., Inagaki, N., and Seino, S. (1997) *J. Biol. Chem. 272*, 22983−22986.
66. InVitrogen, Instruction Manual, *Pichia* Expression Kit, catalog no. K1710-01.
67. Liu, R., and Sharom, F. J. (1996) *Biochemistry 35*, 11865−11873.

BI9728001